Gene-corrected human Munc13-4-deficient CD8$^+$ T-cells can efficiently restrict EBV-driven lymphoproliferation in immunodeficient mice.

Tayebeh Soheili [1,2,3], [*]Julie Rivière [1,2], [*]Ida Ricciardelli [4], Amandine Durand [1,2], Els Verhoeyen [5,6], Anne-Céline Derrien [1,2], Chantal Lagresle-Peyrou [1,2,3], Geneviève de Saint Basile [2,7,8], François-Loïc Cosset [5], Persis Amrolia [4], Isabelle André-Schmutz [1,2] and Marina Cavazzana [1,2,3]

[1]Human Lymphohaematopoiesis Laboratory, INSERM U1163, Paris, France
[2]University of Paris Descartes-Sorbonne Paris Cité, IMAGINE Institute, Paris, France
[3]Biotherapy Clinical Investigation Centre, Necker Children's Hospital, Paris, France
[4]Molecular and Cellular Immunology Unit, Institute of Child Health, London, UK
[5]Centre International de Recherche en Infectiologie, Enveloped Viruses, Vectors and Innate Responses Research Group, Lyon University, Lyon, France
[6]C3M, Inserm, U1065, équipe "contrôle métabolique des morts cellulaires", Nice, 06204, France
[7]Normal and Pathological Homeostasis of the Immune System Laboratory, INSERM U1163, Paris, France
[8]Centre d'Etudes des Déficits Immunitaires, Assistance Publique-Hôpitaux de Paris, Hôpital Necker, Paris, France

*: These authors contributed equally.

Running Title: T-cell gene therapy for FHL type 3

Text word count: **1200**
Number of figures: **2**
Number of references: **22**

Corresponding author:
Isabelle André-Schmutz
INSERM U1163, Imagine Institute
24, Boulevard de Montparnasse
F-75015 Paris
France
Phone: +33 142754337
Fax: +33 142754225
andre.schmutz@gmail.com

Key Points:

- VSVG and H/F lentiviral Munc13-4 gene transfer into FHL3 patients' T-cells restores the latter's *in vitro* degranulation capacity.
- Munc13-4 gene-corrected T-cells efficiently restrict the growth of autologous EBV-lymphoma in immunodeficient mice.

Familial haemophagocytic lymphohistiocytosis type 3 (FHL3) is a hyperinflammatory disease caused by mutations in the *UNC13D* gene (coding for Munc13-4 protein); FHL3 accounts for 30 to 35% of FHL cases [1]. In cytotoxic T-cells (CTLs) and natural killer (NK) cells, Munc13-4 helps to prime perforin-containing, cytotoxic granules before they fuse with the plasma membrane at the immunological synapse [2,3]. In the absence of effective cytotoxicity, antigen-presenting cells continue to stimulate CTLs - leading to massive proliferation of the latter, the excessive production of interferon gamma (IFNγ), macrophage hyperactivation, and tissue infiltration by activated cells. The clinical phenotype is characterized by prolonged fever, hepatosplenomegaly, lymphadenopathy, rashes and oedema [4]. The condition often appears to be triggered by a viral infection (EBV, in particular) [5–7].

Haematopoietic stem cell transplantation (HSCT) is the only available curative option for FHL3; however, the post-treatment overall survival rate is not satisfactory and depends on (i) the disease state prior to HSCT and (ii) the availability of a matched sibling donor [4]. In addition to HSCT, gene therapy of haematopoietic stem cells has been tested as a treatment for FHL2 in a murine model [8,9]. Given that the main defect in FHL disease is cytotoxic dysfunction of mature T-cells, the latter constitute a potentially valuable target for gene therapy approaches. The genetic modification of T-cells has produced remarkable clinical outcomes in cancer immunotherapy and in cases of adenosine deaminase deficiency[10,11]. To investigate the feasibility and efficacy of gene transfer into human FHL3 T-cells as a means of gene therapy for FHL3, we transduced prestimulated patients' T-cells with a measles virus H and F glycoprotein-pseudotyped lentiviral vector (H/F-LV) prior to adoptive transfer in a NSG mouse model bearing Epstein-Barr virus (EBV)-induced lymphoma. The cytotoxic activity of gene-corrected T-cells was restored, as evidenced by an increase in their *in vitro* degranulation capacity and a progressive regression in the mass of EBV lymphoma (due to the efficient homing of functional cytotoxic T-cells *in vivo*). Transduction of T-cells from

patients with FHL3 with a conventional vesicular stomatitis virus-G lentiviral vector (VSVG-LV) also restored the degranulation capacity (albeit with a lower transduction efficiency than H/F-LV). T memory stem cells (T_{SCM}) were also successfully transduced, and maintained their stem characteristics throughout the culture period. The present work is the first to highlight the potential of engineered T-cell gene therapy in a context of FHL.

Activated peripheral blood mononuclear cells (PBMCs) from FHL3 patients were transduced with either H/F-LV at multiplicity of infection (MOI) of 5 or with VSVG-LV at MOI of 5 and 100. Both vectors code for a human Munc13-4/CFP fusion protein (Supplemental Figure 1A).

An evaluation of the transduction efficacy in bulk transduced cells (6 days after transduction) revealed than the mean vector copy number was higher for H/F-LV than for VSVG-LV (2.22 for H/F-LV; 0.15 and 0.35 for VSVG-LV at an MOI of 5 and 100, respectively) and that Munc13-4 mRNA (Figure 1A) and protein (Figure 1B) expression levels were higher in bulk-H/F-LV-transduced cells. The CFP expression on $CD8^+$ gated cells reached a value of 47.8% ± 13 for H/F-LV but only 7.06% ± 2.4 for VSVG-LV at an MOI of 5 and 12.5% ± 2.5 at an MOI of 100 (Figure 1C).

The surface expression of CD107a/b after TCR stimulation (which accompanies the release of cytotoxic granules) indicated that transduced $CD8^+$ T-cells expressing Munc13-4/CFP (Munc13-4/CFP $^+$) had recovered normal (healthy control) levels of granule release capacity (Figure 1D). This result also suggested that the fusion of CFP with Munc13-4 did not alter the protein's functionality.

On the basis of these *in vitro* data, we measured the *in vivo* cytotoxic activity of Munc13-4/CFP-transduced T-cells from FHL3 patients. EBV is one the major infectious triggers of haemophagocytic lymphohistiocytosis (HLH). We therefore decided to test the ability of Munc13-4/CFP-transduced T-cells to eliminate EBV-induced B-cell lymphoma *in vivo*. Briefly, NSG mice were transplanted with a luciferase-expressing, EBV-transformed B

lymphoblastoid cell-line (B-LCL) derived from a FHL3 patient (P5). When tumours were palpable (around 7 days later), NSG mice were transplanted with EBV-specific T-cells from a single FHL3 patient (bulk-transduced with either H/F-LV expressing Munc13-4/CFP or H/F-LV expressing CFP) (Figure 2A). Measurements of CFP expression seven days after transduction (i.e. before the infusion of EBV-T-cells into the mice) showed that up to 55.2% of the cells had been transduced (Figure 2B) and that the Munc13-4 mRNA level was five times higher in bulk-transduced cells than in healthy controls (data not shown). As shown in Figure 2C and D, and as observed previously [14] using the same xenograft model but with a healthy control as a donor, the tumour mass declined progressively and significantly in NSG mice transplanted with Munc13-4/CFP-transduced T-cells. This contrasted with the outcomes in non-transplanted mice and in mice transplanted with CFP-transduced T-cells, in which the tumours continued to grow up to 30 days post-transplantation. Immunostaining and flow cytometry analysis revealed massive lymphocytic tumor infiltration in NSG mice transplanted with Munc13-4/CFP-transduced T cells (Figure 2E and Supplemental Figure 1B). These results clearly demonstrate that transduction with a LV containing the *UNC13D* gene restores not only the expression of Munc13-4 protein but also the *in vitro* granule release capacity and *in vivo* cytotoxic function of T-cells from FHL3 patients.

In a clinical trial of T-cell gene therapy for adenosine deaminase deficiency, the transduced T-cells persisted in the circulation for up to 12 years after infusion [15] as a result of efficient transduction, *in vitro* expansion and the *in vivo* persistence of T_{SCM}. In the present study, we confirmed the presence of T_{SCM} within the T-cell pool from FHL3 patients (Supplemental Figure 2A). We also demonstrated that T_{SCM} were transduced by both H/F- and VSVG-LVs (Supplemental Figure 2B). The proportion of T_{SCM} increased 48h after TCR stimulation and decreased between days 2 and 8 of culture as a result of differentiation into other memory cells. However, a fraction of these T_{SCM} was still detectable at day 8 in both non-transduced

and transduced conditions, whereas no naïve cells were found in the culture (Supplemental Figure 2C).

Our study is the first to highlight the potential of T-cell gene therapy in a context of FHL. Targeting mature T-cells (rather than haematopoietic stem cells) is associated with a lower risk of insertional mutagenesis and cell transformation [16]. However, one of the limitations of this strategy relates to the generally low transductional efficacy of VSVG-LV. The post-HSCT outcome in HLH patients shows that remission is maintained as long as the level of T-cell donor chimerism reaches 10 to 15% [12,13]. The conventional VSVG-LV strategy must therefore be tested in a preclinical murine model, in order to establish whether or not poor *in vitro* T-cell transduction prevents the achievement of this level of chimerism *in vivo*. Another limitation relates to the availability of T-cells as a result of pancytopenia and the manifestations of HLH. Novel anti-inflammatory modalities for IFNγ blockade (such as the JAK1/2 inhibitor ruxolitinib) can reduce inflammation and correct certain manifestations of FHL (such as blood cytopenia) in murine models of FHL [17,18]. Ruxolitinib has already demonstrated clinical efficacy in other inflammatory conditions [19,20]; if approved in HLH patients, this compound could be used as an anti-inflammatory agent for reducing immune system imbalance prior to T-cell immunotherapy.

Acknowledgments

We thank the patients and their relatives for providing samples. We thank the staff at the Immunology and Paediatric Haematology Department at Necker Children's Hospital (Paris, France) and Dr. G. DeAngulo from Nicklaus Children's Hospital (Miami, FL, USA), who provided patient care. This study was funded by the French National Institute of Health and Medical Research (INSERM), the Association Française contre les Myopathies (AFM, Grant 17045), a European Research Council grant (ERC Regenerative Therapy, 269037) and a European Union FP7 grant (CELL-PID, 261387).

Authorship

Contribution: T.S. designed, conducted and analysed data and wrote the manuscript. J.R. and I.R. designed, performed and analysed experiments and read the manuscript. A.D. and A.C.D. performed and analysed experiments. E.V. and F.L.C. provided vectors and read the manuscript. C.L.P. discussed data and reviewed the manuscript for critical content. G.d.S.B. provided certain patient samples and reviewed the manuscript for critical content. P.A. discussed data. I.A.S. designed and supervised the overall research and wrote the manuscript. M.C. designed and supervised the overall research and reviewed the manuscript for critical content.

Conflict of interest disclosures

The authors declare no competing financial interests.

References

1. De Saint Basile G, Ménasché G, Latour S. Inherited defects causing hemophagocytic lymphohistiocytic syndrome. *Ann. N. Y. Acad. Sci.* 2011;1246:64–76.
2. Feldmann J, Callebaut I, Raposo G, et al. Munc13-4 is essential for cytolytic granules fusion and is mutated in a form of familial hemophagocytic lymphohistiocytosis (FHL3). *Cell*. 2003;115(4):461–473.
3. De Saint Basile G, Ménasché G, Fischer A. Molecular mechanisms of biogenesis and exocytosis of cytotoxic granules. *Nat. Rev. Immunol.* 2010;10(8):568–579.
4. Bode SF, Lehmberg K, Maul-Pavicic A, et al. Recent advances in the diagnosis and treatment of hemophagocytic lymphohistiocytosis. *Arthritis Res. Ther.* 2012;14(3):213.
5. Bode SF, Ammann S, Al-Herz W, et al. The syndrome of hemophagocytic lymphohistiocytosis in primary immunodeficiencies: implications for differential diagnosis and pathogenesis. *Haematologica*. 2015;100(7):978–988.
6. Chandrakasan S, Filipovich AH. Hemophagocytic lymphohistiocytosis: advances in pathophysiology, diagnosis, and treatment. *J. Pediatr.* 2013;163(5):1253–1259.
7. Smith MC, Cohen DN, Greig B, et al. The ambiguous boundary between EBV-related hemophagocytic lymphohistiocytosis and systemic EBV-driven T cell lymphoproliferative disorder. *Int. J. Clin. Exp. Pathol.* 2014;7(9):5738–5749.
8. Carmo M, Risma KA, Arumugam P, et al. Perforin gene transfer into hematopoietic stem cells improves immune dysregulation in murine models of perforin deficiency. *Mol. Ther. J. Am. Soc. Gene Ther.* 2015;23(4):737–745.
9. Tiwari S, Hontz A, Terrell CE, et al. High Level of Perforin Expression Is Required for Effective Correction of Hemophagocytic Lymphohistiocytosis. *Hum. Gene Ther.* 2016;
10. Abate-Daga D, Davila ML. CAR models: next-generation CAR modifications for enhanced T-cell function. *Mol. Ther. Oncolytics*. 2016;3:16014.
11. Aiuti A, Vai S, Mortellaro A, et al. Immune reconstitution in ADA-SCID after PBL gene therapy and discontinuation of enzyme replacement. *Nat. Med.* 2002;8(5):423–425.
12. Gholam C, Grigoriadou S, Gilmour KC, Gaspar HB. Familial haemophagocytic lymphohistiocytosis: advances in the genetic basis, diagnosis and management. *Clin. Exp. Immunol.* 2011;163(3):271–283.
13. Hartz B, Marsh R, Rao K, et al. The minimum required level of donor chimerism in hereditary hemophagocytic lymphohistiocytosis. *Blood*. 2016;
14. Ricciardelli I, Blundell MP, Brewin J, et al. Towards gene therapy for EBV-associated posttransplant lymphoma with genetically modified EBV-specific cytotoxic T cells. *Blood*. 2014;124(16):2514–2522.
15. Biasco L, Scala S, Basso Ricci L, et al. In vivo tracking of T cells in humans unveils decade-long survival and activity of genetically modified T memory stem cells. *Sci. Transl. Med.* 2015;7(273):273ra13.
16. Wu C, Dunbar CE. Stem cell gene therapy: the risks of insertional mutagenesis and approaches to minimize genotoxicity. *Front. Med.* 2011;5(4):356–371.
17. Das R, Guan P, Sprague L, et al. Janus kinase inhibition lessens inflammation and ameliorates disease in murine models of hemophagocytic lymphohistiocytosis. *Blood*. 2016;127(13):1666–1675.
18. Maschalidi S, Sepulveda FE, Garrigue A, Fischer A, de Saint Basile G. Therapeutic effect of JAK1/2 blockade on the manifestations of hemophagocytic lymphohistiocytosis in mice. *Blood*. 2016;
19. Punwani N, Scherle P, Flores R, et al. Preliminary clinical activity of a topical JAK1/2 inhibitor in the treatment of psoriasis. *J. Am. Acad. Dermatol.* 2012;67(4):658–664.
20. Verstovsek S, Kantarjian H, Mesa RA, et al. Safety and efficacy of INCB018424, a JAK1 and JAK2 inhibitor, in myelofibrosis. *N. Engl. J. Med.* 2010;363(12):1117–1127.
21. Frecha C, Costa C, Nègre D, et al. Stable transduction of quiescent T cells without induction of cycle progression by a novel lentiviral vector pseudotyped with measles virus glycoproteins. *Blood*. 2008;112(13):4843–4852.
22. Savoldo B, Goss J, Liu Z, et al. Generation of autologous Epstein-Barr virus-specific cytotoxic T cells for adoptive immunotherapy in solid organ transplant recipients. *Transplantation*.

2001;72(6):1078–1086.

Figure legends

Figure1. *In vitro* restoration of Munc13-4 expression and cytotoxic function after gene transfer into Munc13-4-deficient T-cells. (A) Dot plots represent (for $CD8^+$ gated cells) the number of Munc13-4/CFP^+ cells as a percentage of the $CD8^+$ population six days after transduction with H/F-LV at an MOI of 5 or with VSVG-LV at an MOI of 5 and 100. The experiments were performed on three different FHL3 samples (P5, P6, and P7); one representative experiment is shown. (B) The level of Munc13-4 mRNA expression was 4.4 to 5.5 times higher in the patients' H/F-LV-bulk-transduced cells than in healthy controls and non-transduced FHL3 cells, and was 1.5 times higher in VSVG-LV-transduced cells (MOI: 100) than in non-transduced cells (in the same three samples as above). The data were normalized against *GAPDH* and are expressed as a fold-change relative to healthy control T-cells. It is noteworthy that mRNA levels were similar in non-transduced patient cells and healthy control cells. (C) Munc13-4 protein expression 6 days after transduction (in the same three samples as above; only P6 and P7 are presented here). (D) The number of CD107a/b^+ cells as a percentage of the $CD8^+$ T-cell population after stimulation with 30 µg/ml anti-CD3. In transduced samples, the percentage of CD107a/b^+ cells are presented with respect to CFP^+ or Munc13-4/CFP^+ gated cells. n=7 different FHL3 samples for non-transduced cells (P1 to P7), n=5 for H/F-CFP as a control (P3 to P7), n=3 for H/F (P5 to P7); n=6 for VSVG experiments (P1 to P3, P5 to P7). Data are presented as the mean ± standard deviation (SD). *P* values were calculated using an unpaired *t*-test for mRNA expression and a two-sided Mann-Whitney test for CD107a/b surface expression in the degranulation assay. *$p<0.05$, *ns*=non-significant.

Figure 2. Adoptive transfer of Munc13-4-corrected EBV-specific T-cells induces the regression of EBV B-cell lymphoma in NSG mice. (A) Experimental design for the xenograft NSG mouse model. The experiment was performed with PBMCs from P5 (an EBV-seropositive patient). N=3 mice per group. B-LCL: B-lymphoblastoid cell line. (B) The dot plot represents the number of Munc13-4/CFP^+ cells as a percentage of the $CD8^+$-gated population 7 days after transduction. (C) Bioimmunoluminescence imaging using the IVIS *in vivo* imaging system (Xenogen; Caliper Life

Sciences, Hopkinton, MA) for NSG mice bearing EBV B-cell lymphoma. EBV-T-cells: EBV-specific cytotoxic T-cells. (D) The time course of tumor growth. Photon emission from luciferase-positive tumour cells was quantified as the peak photons/sec/cm^2/steradian (p/s/cm^2/sr). Error bars represent the mean ± standard error of the mean (SEM). The *p* value was calculated in a two-way analysis of variance with a Bonferroni post-test (E) The percentage of human $CD3^+$ T-cells and luciferase-expressing lymphoma cells in digested tumours, as measured by flow cytometry. The mean cell count ± SD is shown. The *p* value was calculated in an unpaired *t*-test. *$p<0.05$, **$p<0.01$, ***$p<0.001$.

Figure 1.

A.

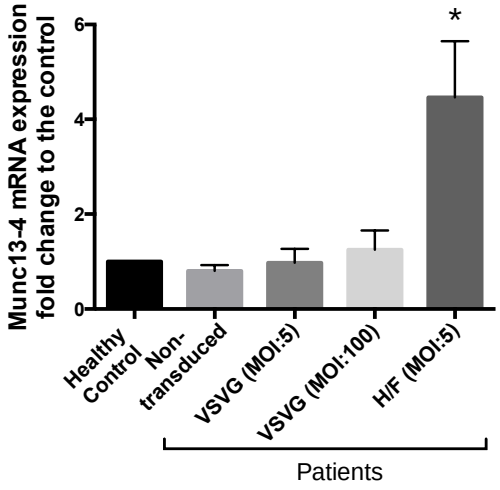

B.

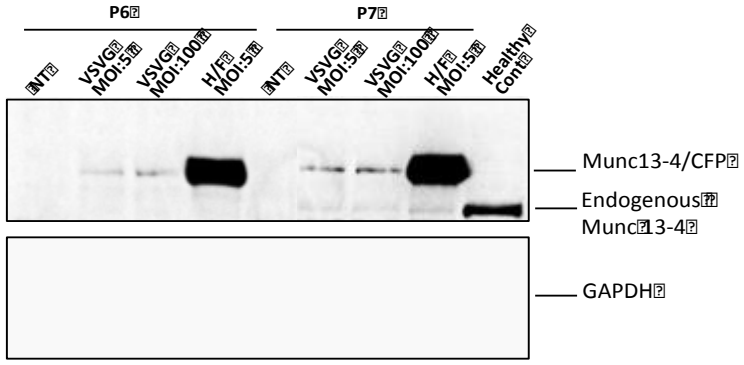

C.

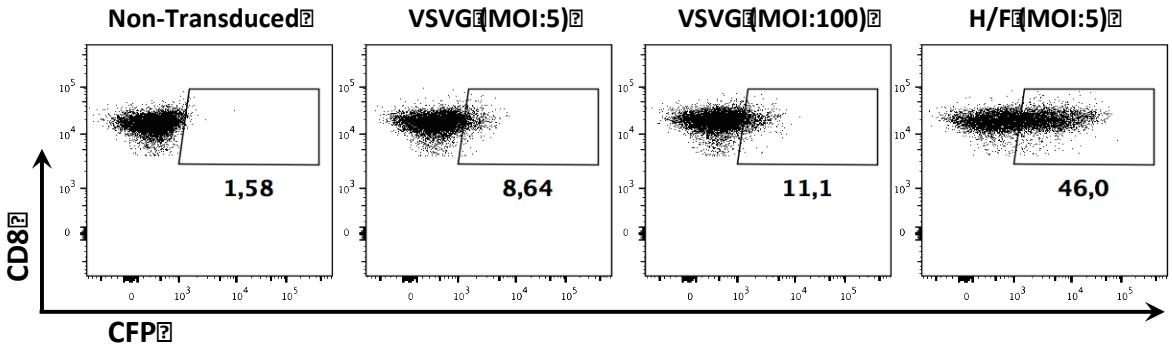

D.

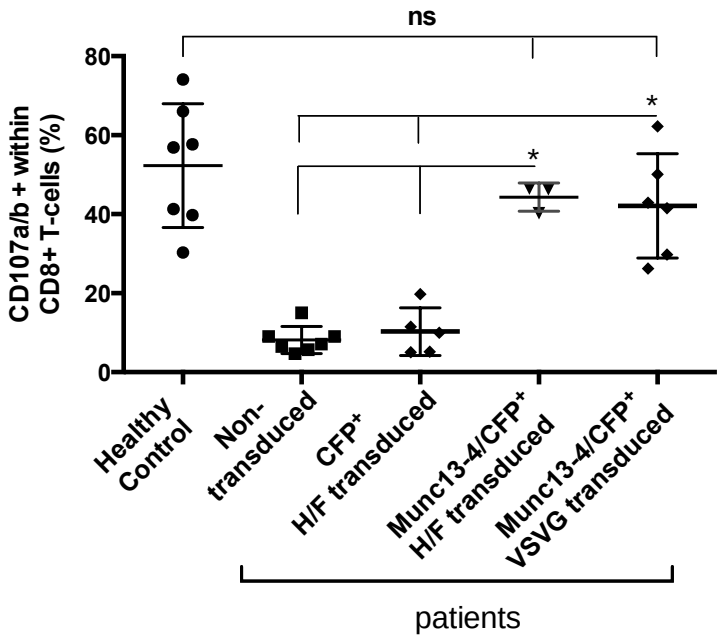

Figure 2.

A.

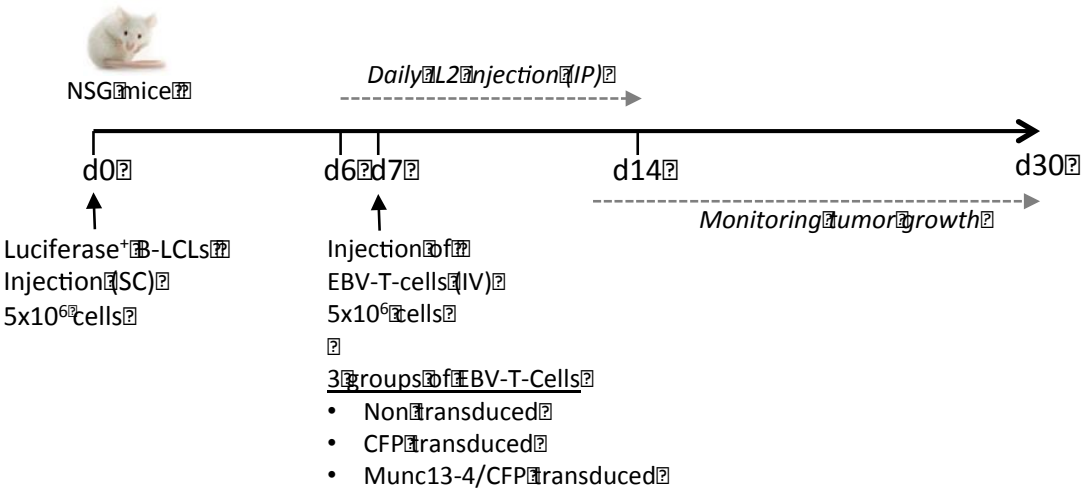
NSG mice
Daily IL2 injection (IP)
d0
d6
d7
d14
d30
Monitoring tumor growth
Luciferase+ B-LCLs
Injection (SC)
5x10^6 cells
Injection of
EBV-T-cells (IV)
5x10^6 cells
3 groups of EBV-T-Cells
Non transduced
CFP transduced
Munc13-4/CFP transduced

B.

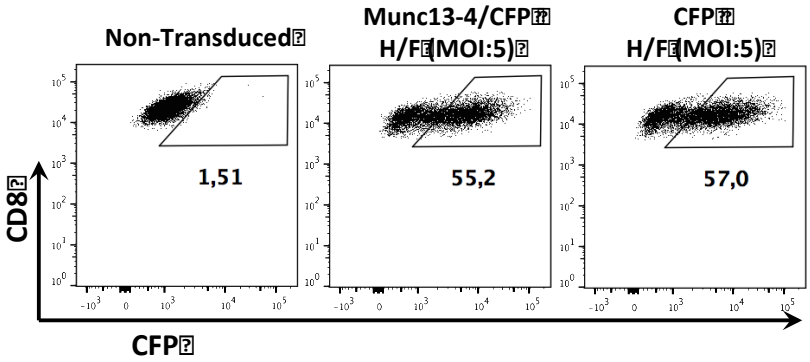
Non-Transduced
Munc13-4/CFP
H/F (MOI:5)
CFP
H/F (MOI:5)
1,51
55,2
57,0
CD8
CFP

C.

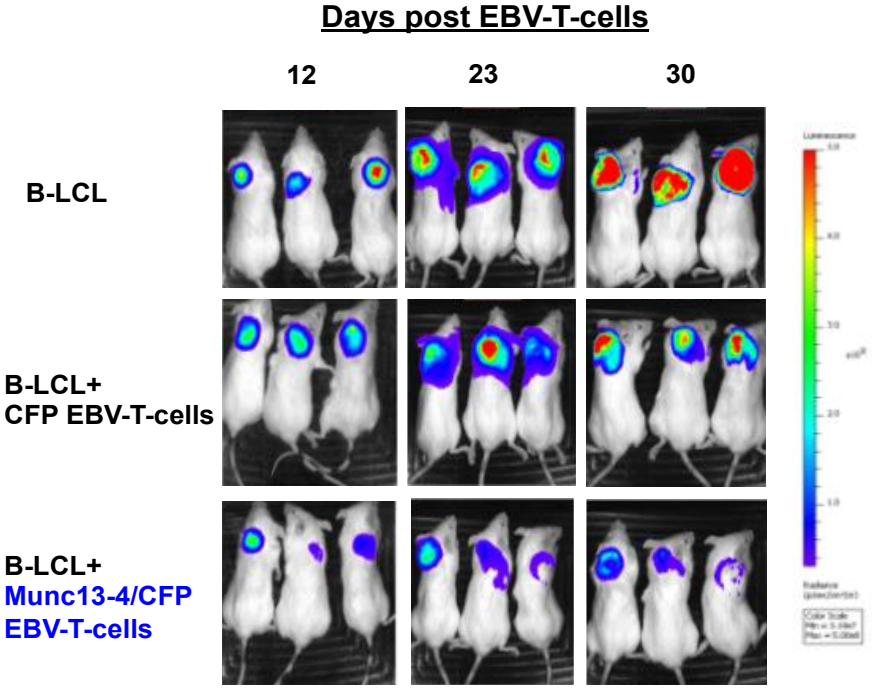
Days post EBV-T-cells
12
23
30
B-LCL
B-LCL+
CFP EBV-T-cells
B-LCL+
Munc13-4/CFP
EBV-T-cells

D.

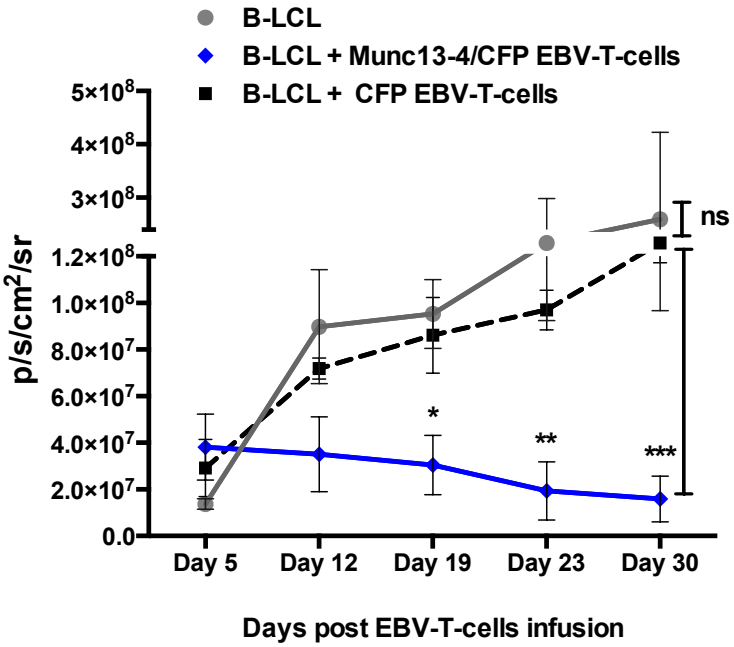
B-LCL
B-LCL + Munc13-4/CFP EBV-T-cells
B-LCL + CFP EBV-T-cells
5×10^8
4×10^8
3×10^8
1.2×10^8
1.0×10^8
8.0×10^7
6.0×10^7
4.0×10^7
2.0×10^7
0.0
p/s/cm^2/sr
ns
*
**
***
Day 5
Day 12
Day 19
Day 23
Day 30
Days post EBV-T-cells infusion

E.

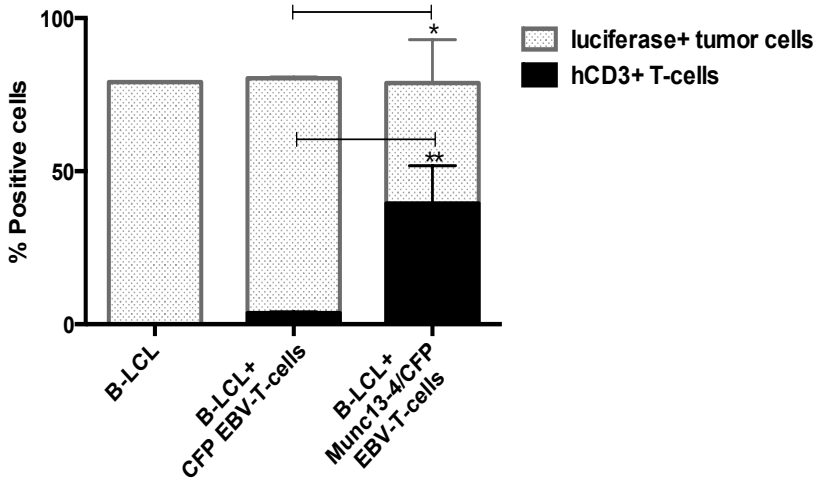
100
50
0
% Positive cells
*
**
luciferase+ tumor cells
hCD3+ T-cells
B-LCL
B-LCL+ CFP EBV-T-cells
B-LCL+ Munc13-4/CFP EBV-T-cells